Physical Chemistry Chemical Physics c6cp03234f

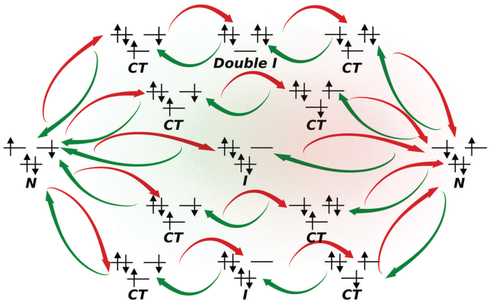

Q3

Highly efficient perturbative + variational strategy based on orthogonal valence bond theory for the evaluation of magnetic coupling constants. Application to the trinuclear Cu(II) site of multicopper oxidases

Lorenzo Tenti,* Daniel Maynau, Celestino Angeli and Carmen J. Calzado*

A new *perturbative + variational* strategy: a low-cost, quantitative and rational evaluation of the magnetic coupling constant in complex systems.

Queries for the attention of the authors

Journal: **PCCP**

Paper: **c6cp03234f**

Title: **Highly efficient perturbative + variational strategy based on orthogonal valence bond theory for the evaluation of magnetic coupling constants. Application to the trinuclear Cu(II) site of multicopper oxidases**

Editor's queries are marked on your proof like this Q1, Q2, etc. and for your convenience line numbers are indicated like this 5, 10, 15, ...

Please ensure that all queries are answered when returning your proof corrections so that publication of your article is not delayed.

Query reference	Query	Remarks
Q1	For your information: You can cite this article before you receive notification of the page numbers by using the following format: (authors), Phys. Chem. Chem. Phys., (year), DOI: 10.1039/c6cp03234f.	
Q2	Please carefully check the spelling of all author names. This is important for the correct indexing and future citation of your article. No late corrections can be made.	
Q3	The title has been altered for clarity, please check that the meaning is correct.	
Q4	Please check whether affiliation c has been presented correctly and indicate any changes that are required.	
Q5	The sentence beginning "Once a reduced set of excitations..." has been altered for clarity, please check that the meaning is correct.	
Q6	The sentence beginning "This approach provides evidence for..." has been altered for clarity, please check that the meaning is correct.	
Q7	The sentence beginning "The use of localized orthogonal orbitals..." has been altered for clarity, please check that the meaning is correct.	
Q8	The sentence beginning "In simple words, the definition..." has been altered for clarity, please check that the meaning is correct.	
Q9	The sentence beginning "Alternatively, it is possible to rely on the minimal..." has been altered for clarity, please check that the meaning is correct.	
Q10	The sentence beginning "Hence, the Goodenough mechanism, usually..." has been altered for clarity, please check that the meaning is correct.	
Q11	The sentence beginning "It is worth noting that this small number..." has been altered for clarity, please check that the meaning is correct.	
Q12	The sentence beginning "Regarding the two molecular systems considered..." has been altered for clarity, please check that the meaning is correct.	
Q13	The sentence beginning "Once this issue has been addressed, the..." has been altered for clarity, please check that the meaning is correct.	

PCCP

PAPER

Cite this: DOI: 10.1039/c6cp03234f

Highly efficient perturbative + variational strategy based on orthogonal valence bond theory for the evaluation of magnetic coupling constants. Application to the trinuclear Cu(II) site of multicopper oxidases† Q1 Q3

Lorenzo Tenti,*[a] Daniel Maynau,[b] Celestino Angeli[a] and Carmen J. Calzado*[c]

A new strategy based on orthogonal valence-bond analysis of the wave function combined with intermediate Hamiltonian theory has been applied to the evaluation of the magnetic coupling constants in two AF systems. This approach provides both a quantitative estimate of the *J* value and a detailed analysis of the main physical mechanisms controlling the coupling, using a combined *perturbative + variational* scheme. The procedure requires a selection of the dominant excitations to be treated variationally. Two methods have been employed: a brute-force selection, using logic similar to that of the CIPSI approach, or entanglement measurements, which identify the most interacting orbitals in the system. Once a reduced set of excitations (about 300 determinants) is established, the interaction matrix Q5 is dressed at the second-order of perturbation by the remaining excitations of the CI space. The diagonalization of the dressed matrix provides *J* values in good agreement with experimental ones, at a very low-cost. This approach provides evidence for the key role of d → d* excitations in the quantitative Q6 description of magnetic coupling, as well as the importance of using an extended active space, including the bridging ligand orbitals, for the binuclear modelling of the intermediates of multicopper oxidases. The method is a promising tool fro dealing with complex systems containing several active centers, as an alternative to both pure variational and DFT approaches.

Received 12th May 2016,
Accepted 8th June 2016

DOI: 10.1039/c6cp03234f

www.rsc.org/pccp

1 Introduction

The rationalization of the physical mechanisms controlling the interaction between unpaired electrons in magnetic systems has been a matter of study in molecular magnetism for decades. Driven by this aim, different models have been proposed to interpret magnetic coupling, including that of Anderson[1] in the solid state physics domain, and the models introduced by Kahn and Briat,[2] and Hay, Thibeault and Hoffmann[3] conceived for magnetic transition metal complexes. Mainly devoted to the study of binuclear complexes with $S = 1/2$ centers, these models only took into account the unpaired electrons occupying the magnetic orbitals, a and b, and their success resides in providing simple expressions for the magnetic coupling constant J on the basis of a reduced number of parameters; K_{ab}, t_{ab} and U, where K_{ab} is the direct exchange between the active orbitals, t_{ab} is the hopping integral between the magnetic centres and U is the energy difference between the ionic forms, with two electrons in the same magnetic center, and the neutral forms, containing one unpaired electron per magnetic site.

These models have been successful in qualitatively describing the nature of the interaction but soon after de Loth *et al.*[4] showed that these *active-electron-only* approximations are not able to provide J values in agreement with the experiment, J being in general at least one order of magnitude too small or even of incorrect sign, and many subsequent applications have corroborated this.[5–10] Indeed, the seminal work by de Loth *et al.* provided evidence that the other electrons play a key role in magnetic coupling by means of different processes such as hole and particle polarization, spin polarization, ligand to metal and metal to ligand charge transfer (LMCT and MLCT), and combined (higher order) effects. They have proposed an expression of J based on second-order perturbation theory (PT), which only

[a] *Dipartimento di Scienze Chimiche e Farmaceutiche, Università degli Studi di Ferrara, Via Fossato di Mortara 17, 44121 Ferrara, Italy. E-mail: lorenzo.tenti@unife.it*

[b] *Laboratoire de Chimie et Physique Quantique, IRSAMC, Université de Toulouse, 118, route de Narbonne, 31062 Toulouse, France*

Q4 [c] *Departamento de Química Física, Universidad de Sevilla, c/Prof. García González, s/n. 41012, Sevilla, Spain. E-mail: calzado@us.es*

† Electronic supplementary information (ESI) available. See DOI: 10.1039/c6cp03234f

takes into account the differential effect playing a role on the energy difference between the states involved in the coupling. The procedure has been useful for rationalizing the magnetostructural behaviour of several Cu(II) binuclear compounds,[6,11,12] and it has been quickly surpassed by a variational version, the difference dedicated configuration interaction (DDCI) approach by Malrieu and coworkers,[13,14] which ensures the introduction of higher-order effects and avoids the intrinsic convergence problems of the perturbation expansion. The first DDCI calculation was carried out by Broer and Maaskant[15] with the aim of analyzing magnetostructural correlations in the $[Cu_2Cl_6]^{-2}$ complex. From then on, the DDCI approach has been particularly successful in the quantitative evaluation of magnetic coupling constants in many solid and molecular magnetic systems[16] and at present it is considered as the reference method in this field.

The possibility of accessing quantitative estimations of J using the DDCI method has renewed interest in the rationalization of magnetic interactions and stimulated a series of works dedicated to the analysis of the physical effects governing coupling at the DDCI level.[17–19] The DDCI space contains different classes of determinants, characterized by the number of inactive doubly occupied (holes, h) and virtual (particles, p) orbitals involved in the excitation. Among all excitations in the DDCI space, those carrying the largest effect on the coupling constant are the 1h1p determinants (responsible for the stabilization of the ionic forms and the introduction of spin polarization mechanisms) and the 2h1p and 1h2p excitations, which contribute to a large fraction (30–50%) of the coupling. The 2h1p determinants only bring a small antiferromagnetic contribution when acting directly on the CAS space, far removed from the large effect found at the DDCI level. This suggests that their impact is not related to a direct coupling with the ionic and neutral forms (second- and third-order effects), but that it must be mediated by indirect coupling through other electronic configurations (a higher-order effect). This proposal has been supported by a series of class-partitioned CI calculations where the variational space is step-by-step increased by different classes of excitations.[19] Meticulous analysis of the so-obtained J values supports a complex mechanism where the 2h1p excitations acquire their key role only in presence of the LMCT and 1h1p determinants. The origin of this cooperative effect could be related to a stabilization of the ionic and LMCT configurations due to the 2h1p and 1h1p excitations, resulting in a remarkable amplification of the AF character of J.

It is worth noting that this analysis has been performed on wave functions based on the triplet CASSCF molecular orbitals (MOs) expanded in a minimal CAS. It takes into account the relative energy of the intermediates generated on this basis, and the amplitude of the interaction terms following arguments such as Brillouin's theorem. The use of the singlet CASSCF MOs only marginally modifies the scheme reported. However, if DDCI natural orbitals are employed, for which magnetic orbitals are more delocalized on the ligands than the CASSCF ones,[20] both the excitation energies and the interaction terms are affected. Hence, the relative importance of each interaction pathway on the magnetic coupling is also revised, some pathways that are negligible on the basis of canonical MOs become dominant, while others appear to contribute at a lower order of perturbation.

In this work we provide *direct* and *numerical* evidence for the cooperative effect introduced by 2h1p excitations and the whole set of mechanisms controlling the magnetic coupling. Based on the orthogonal valence bond (OVB) reading of the wave function and the use of the intermediate Hamiltonian theory, a rational strategy is proposed to analyze and finally *quantify* the physical effects in terms of the modification of some interaction terms and the lowering of the effective energy of those configurations strongly affecting the coupling.

This strategy provides guidance for classifying the determinants that are able to provide a quantitative estimate of J on two groups, those that need to be treated variationally and those whose effect can be introduced by perturbation. The former group contains a reduced number of excitations (less than 0.05% of the whole space), those with a large interaction with the model space or those with a large impact on the effective energies of the determinants in the model space. The resulting CI matrix is dressed by the effect of the excitations belonging to the second group using second-order PT. This *perturbative + variational* strategy could be a powerful tool for dealing with large and complex polynuclear magnetic systems, combining the benefits of the variational methods and the low-cost requirements and high performance of the perturbation approach. To illustrate this strategy, two antiferromagnetic systems have been considered here, a binuclear model related to one of the native intermediates of the multicopper oxidases cycle (*vide infra*) and a binuclear Cu(II) complex, with similar ligands in the metal coordination spheres.

2 Description of the systems and computational details

Two antiferromagnetic binuclear Cu(II) systems have been considered. Their geometries have been taken from X-ray crystal data[21,22] and are shown in Fig. 1.

The system referred to as bisOH in Fig. 1 can be obtained from the tris(μ-hydroxy)tricopper(II) complex, $[Cu_3(dbed)_3(\mu\text{-}OH)_3](ClO_4)_3$ (trisOH), by substitution of a Cu atom with a Zn atom. The trinuclear complex trisOH is a bio-mimetic

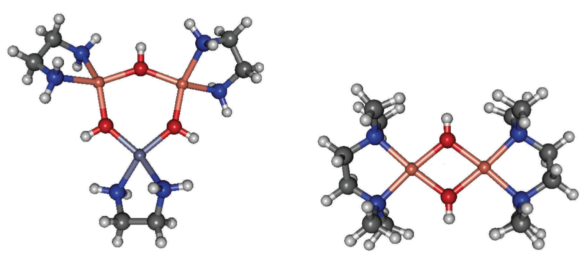

(a) bisOH (b) $Cu_2(OH)_2$

Fig. 1 Geometries of the systems here considered.

compound that models one of the native intermediates of the multicopper oxidases catalytic cycle.[22–25] In this complex, with rigorous D_3 symmetry, the Cu centers are arranged in a triangle, connected to each other by an hydroxo group. The Cu–OH–Cu angle is 140.5° and the Cu–OH distance is 1.96 Å. The bidentate *N*,*N'*-di-*tert*-butylethylendiamine (dbed) ligand completes the coordination sphere of each metal atom. The magnetic interaction between the Cu(II) centers in the trimeric complex is antiferromagnetic, resulting in a spin-frustrated two-fold (four-fold considering the spin degeneracy) degenerate doublet ground state. In the frame of the isotropic exchange Heisenberg–Dirac–Van Vleck (HDVV) Hamiltonian,[26–28]

$$\hat{H}_{\text{Heis}} = -\sum_{i<j} J_{ij}\hat{S}_i \cdot \hat{S}_j \qquad (1)$$

these degenerate ^{2}E doublet states are separated by an energy of $3J/2$ from the quartet state $^4A_2$. The fitting of the magnetic susceptibility data[22] yields a J value of $\approx -210\ \text{cm}^{-1}$ and then a doublet–quartet splitting energy of $3J/2 \approx -315\ \text{cm}^{-1}$. The EPR and variable-temperature variable-field magnetic circular dichroism (VTVH MCD) spectra demonstrate the existence of the competing effects of antisymmetric exchange and symmetry lowering, in addition to the dominant isotropic exchange coupling. These terms are important for explaining the observed magnetic and spectroscopic data at low temperature.[23]

The electronic structure and EPR g tensors of the trisOH system together with many other inorganic models of the trinuclear Cu(II) sites of multicopper oxidases have been previously studied by multireference *ab initio* calculations,[29] including CASPT2, MS-CASPT2, DDCI and MRCI calculations. As the authors claimed, these multireference methods only yield qualitatively correct results, the main issue being the correct description of the relative energies of the ground doublet and the excited quartet states. Table 1 collects the doublet–quartet gap (Δ) and J values obtained by Vancoille *et al.*[29] for trisOH. In general, the calculated CASPT2 values of the magnetic coupling constant are lower than the experimental ones, while DDCI largely overestimates the doublet–quartet gap. The inclusion of the spin–orbit coupling effect only modifies the J values by a few wavenumbers. As the authors noticed, the underestimation of the CASPT2 values is somewhat expected, but the large overestimation of the DDCI values is *highly unusual* for this method.

Table 1 Variational and perturbation estimates from ref. 29 of the doublet–quartet gap, Δ, and magnetic coupling constant, J, (in cm^{-1}) for the trisOH system

	Δ	$J = 2\Delta/3$
Exp.	−315	−210
CASSCF(27,15)/CASPT2	−105	−70
CASSCF(27,15)/CASPT2/MS-CASPT2	−112	−75
DDC2(3,3)	−875	−583
DDCI(3,3)	−718	−479

In the present study we focus on the evaluation of the isotropic exchange coupling constant J. For this purpose, a simplified binuclear bisOH model is employed, where one of the Cu(II) atoms is replaced by a diamagnetic Zn(II) ion. To reduce the computational cost, the external *tert*-butyl groups are replaced by H, with a fixed N–H distance of 1.02 Å.

The second system explored, named $Cu_2(OH)_2$ in Fig. 1, consists of two Cu(II) centers bridged by two hydroxo groups, $[Cu(tmen)OH]_2Br_2$. The Cu atoms present a square-planar coordination, where the Cu–O–Cu angle is 104.1° and the Cu–OH distance is 1.90 Å. The coordination sphere is completed with tmen (*N*,*N*,*N'*,*N'*-tetramethylethylenediamine).[21] The two Cu(II) centers show strong antiferromagnetic coupling with $J = -509\ \text{cm}^{-1}$, relative to the HDVV Hamiltonian.[21]

Both systems contain only two active $S = 1/2$ antiferromagnetically coupled centers and J can be evaluated from the singlet–triplet energy difference, $J = E(S) - E(T)$. For the sake of comparison, for both systems we have used the basis sets employed in ref. 29: the ANO-S basis sets with contraction [6s4p3d2f] for Cu and Zn atoms, [3s2p1d] for O, N and C atoms, and [2s] for H atoms. All CASSCF calculations have been performed using the MOLCAS 7.8 program package.[30] The OVB analyses[31–33] were made with *ad hoc* codes developed by the Ferrara group. The CASDI[34,35] code has been used for DDCI calculations.

Several sets of MOs have been employed, both delocalized and localized. As will be discussed later, the DDCI calculations show a strong dependence on the MOs, in contrast to what is usually expected. The common strategy based on the use of CASSCF orbitals optimized for the triplet state is unable to well describe the physics of the systems considered here. A set of natural orbitals (obtained from the diagonalization of the average singlet and triplet DDCI one-particle density matrices) allows one to overcome this problem.

3 Method

In the following, the two main methods used in this work, the orthogonal valence-bond and the intermediate Hamiltonian approaches, are briefly outlined. In addition, a few details are provided regarding the localization method.

3.1 The orthogonal valence-bond method

The main aim of the OVB method is to combine, in an optimal way, the effectiveness and computational efficiency of the MO approach with the interpretative potential of the valence-bond (VB) method.

The VB approach played a fundamental role in the dawn of modern theoretical chemistry, but quickly faced the problem of an explosion of the number of structures, that, along with their non-orthogonal nature, has made this method highly computationally demanding, at least when compared with the rising MO theory. The delocalized MO picture, indeed, has offered an extremely efficient tool for the calculation of ionization and excitation processes and has rapidly become a standard method in the field, leaving the VB method to a niche of users. However, the VB method is not only a method for computing approximate wave functions and energies, but is also a tool for analyzing the electronic structure from a point of view that is close to the chemist's way of thinking, through the use of Lewis' concepts concerning bonds and lone pairs.[36,37]

Staying within the MOs framework, it is important to note that the core, active and virtual delocalized MOs obtained from a standard CASSCF approach can be rotated among themselves and transformed into localized orbitals, leaving the CASSCF wave function and its properties unchanged.[38] For active space the flexibility of the localization procedure is maximum if a full valence active space is used: two interesting possibilities are orthogonal atomic orbitals (OAOs) and localized molecular orbitals (LMOs), the latter essentially describing bonding and antibonding orbitals, lone pairs, *etc.* The possibility of transforming delocalized MOs to localized OAOs or LMOs shows the perfect compatibility between the MO, VB and Lewis pictures and allows one to perform a VB-type reading of a correlated MO wave function. One of the peculiarities of this approach, when compared with traditional VB procedures, is the use of orthogonal orbitals. For this reason, the method is called the orthogonal valence-bond method.

Q7 The use of localized orthogonal orbitals (in particular OAOs) as building blocks for the study of VB-like electronic molecular structures has recently received theoretical foundation following a deep analysis on the simple H_2 molecule,[32] in particular due to the possibility of associating a given OVB structure with a well defined nature.[33] Indeed, the orthogonality of the monoelectronic functions, and therefore of the Slater determinants from those obtained, is not only a technical concern but involves a deeply different interpretation of the nature of the chemical bond[32] and in general of the electronic structure.[39–41]

The OVB reading of a wave function, already very interesting by itself, draws further interest when a few relevant VB-like structures are identified (defining a model space) and the Hamiltonian matrix in such a space is dressed by the effect of the rest of the CI space. In this way, one can include a dynamical correlation of the electrons by considering the effective energies and interactions within the model space. This procedure is used in the present work, performing a VB reading of the DDCI wave function (or a subspace of this function) using localized orbitals in agreement with Lewis' structures and considering the theory of the intermediate Hamiltonians for the dressing, shortly described in Section 4.3.

3.2 The Lewis localization method

Several methods can be found in literature for the generation of localized orbitals optimized at the mean field level (both single reference or multireference). In most of them, the MOs are firstly optimized in a standard procedure and the final canonical (delocalized) MOs are then localized. To this aim, most of the localization methods[42–44] use an intrinsic criterion of localization, in general by maximizing some localization function, while other localization procedures are based on an extrinsic criterion, as, for instance, the projection of localized MOs on the canonical SCF ones. The method employed in this article belongs to the latter group, in which a set of strongly localized (not optimized) MOs built using the Lewis method (*vide infra*) is projected on a set of optimized MOs.

In the Lewis approach, the first step is to build a set of (non optimized) localized orbitals. The procedure starts with a representation of the molecule following the idea of the Lewis structures, where different kinds of orbitals appear. One may identify bonding and anti-bonding orbitals between neighbouring atoms, atom-centered doubly occupied orbitals (as, for instance, core orbitals) and unoccupied diffuse orbitals. The lone pairs can also be considered as atom-centered orbitals. Moreover, orbitals involving more than two atoms may be considered, such as partially delocalized π (occupied or not) orbitals distributed on a small part of the molecule. The user must build all core and valence orbitals, while the virtuals are automatically generated by the program as atom-centered orbitals. In summary, this step corresponds to a thorough analysis of the system studied and is thus far removed from looking like a black box. Indeed, a large degree of freedom is given to the user who, in the end, is required to have a good understanding of the chemical nature of the molecule.

The guess local (non orthogonal) orbitals are orthogonalised through a hierarchical orthogonalisation method, which consists of a series of $S^{-1/2}$ and projection (Gram-Schmidt) steps. The first priority is given to the core orbitals, as they are responsible for the largest part of the energy of the system. They are orthogonalised among themselves through a $S^{-1/2}$ procedure. The second class corresponds to the active orbitals. They are projected on the space complementary to the space spanned by the core orbitals (Gram-Schmidt projection) and orthogonalised among themselves through a $S^{-1/2}$ transformation. The next class is the valence class and, finally, the virtual orbital class, for which a similar strategy is applied.

Once the guess local orthogonal orbitals are generated, they can be used as a starting point for a CASSCF calculation[45] or projected on an optimized set of MOs, the CASSCF MOs or the natural DDCI MOs, as it is the case in this work. Each orbital space (doubly occupied, active, and virtual) is projected separately. Compared to a localization method based on an intrinsic criterion, for which a simple keyword is enough to get a set of localized orbitals, the Lewis approach is more demanding for the user, even if it is computationally very efficient. One must however emphasize that all orbitals can be localized without difficulty, in particular the virtual ones. Indeed, the localization criteria appearing in the most diffused methods require, in general, the presence of electrons in the orbitals, so localizing the virtual MOs can be difficult. Finally, the application of methods based on intrinsic criteria can give orbitals that, even if they have a small spatial extension and they are therefore local, do not correspond to bonds, lone pairs, or any of the orbitals typical of the Lewis description. The advantage of working with orbitals that exactly correspond to the Lewis description of the molecular architecture is helpful in particular from a VB logic, as will be evident in the following.

3.3 The intermediate Hamiltonian theory

As reported previously, the DDCI method takes into account the most important physical effects governing magnetic coupling. Nevertheless, understanding the nature of this wave function is not straightforward, due to its highly multiconfigurational nature. The most rigorous way to return to the simplicity of the one or two-bands model (or of other more refined models) is to make use of the effective Hamiltonian theory.[46,47] For the study of magnetic coupling, only the first few roots of the full DDCI Hamiltonian matrix are required and one can resort to the less ambitious theory of the intermediate Hamiltonians.[48]

The intermediate Hamiltonian theory is based on the partition of the CI space in a model space, S_0, and its orthogonal counterpart $S_0^{\perp}$, the outer space. The model space is further partitioned into a main model space, S_m, of dimension N_m, and Q8 an intermediate space, S_i, of dimension N_i. In simple words, the definition of the intermediate Hamiltonian is based on the idea of bringing together information from the model space and the CI space required to describe N_m FCI wave functions in the best possible way. The intermediate Hamiltonian can be built through the use of perturbation theory. For the special case of N_m = 1, relevant for the problems considered in this work, the matrix elements of the second order perturbation correction of H in the model space are

$$\left\langle i \middle| H_{\mathrm{int}}^{(2)} \middle| j \right\rangle = \sum_{\alpha} \frac{\langle i|V|\alpha\rangle\langle\alpha|V|j\rangle}{E_0 - E_\alpha^0} \quad (2)$$

where i and j are in the model space and α is in the outer space. In this way, one dresses the true Hamiltonian in S_0 with the effect of the outer space. The diagonalization of the dressed Hamiltonian matrix relative to the model space (of dimension N_m + N_i) provides N_m eigenvalues and eigenstates, which approximate at best to the corresponding exact quantities, and N_i solutions, which is a lower approximation than the exact ones. Here N_m = 1 and in principle only the lowest state is correctly treated. However, noticing that the lowest singlet and triplet states are almost degenerate (at least with respect to the value of the energy differences in the denominators of eqn (2)), one can consider both states in an optimal way using the energy of one of the two states or the average of their energies for E_0, as is the case in this work.

4 Results and discussion

4.1 Difference dedicated CI results

The common approach for evaluation of J in systems with two unpaired electrons is based on the use of triplet CASSCF MOs, where the active space contains the singly occupied 3d orbitals of the metallic centers (or in-phase and out-of-phase combinations of them). These orbitals are not purely atomic given that they show tails on the surrounding ligands. Afterwards, the application of the DDCI method on this minimal active space usually gives J values in good agreement with the experimental data (see for instance, ref. 16 and references therein).

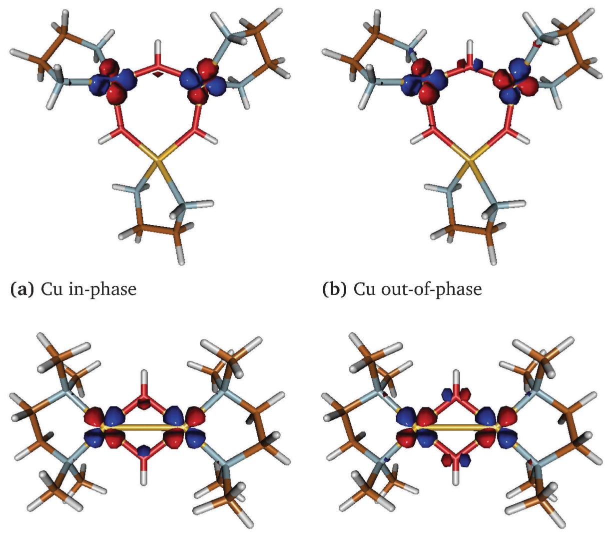

(a) Cu in-phase **(b)** Cu out-of-phase **(c)** Cu in-phase **(d)** Cu out-of-phase

Fig. 2 Triplet CASSCF(2,2) active orbitals for bisOH (a and b) and $Cu_2(OH)_2$ (c and d).

Fig. 2 shows the triplet CASSCF(2,2) active orbitals for bisOH and $Cu_2(OH)_2$. In both cases, they have dominant Cu $3d_{x^2-y^2}$ character. For the $Cu_2(OH)_2$ system, each Cu center adopts square-planar coordination, and the $3d_{x^2-y^2}$ orbitals are in the same plane of the OH bridges. In contrast, in the bisOH system, the Cu coordination polyhedra are distorted with respect to the square-planar one, with the two N atoms slightly rotated out of the plane containing the Cu atoms and the OH ligands (tetrahedral distortion). As a result, the active $3d_{x^2-y^2}$ orbitals are not in the same plane. Actually, the active orbitals are not strictly speaking $3d_{x^2-y^2}$ orbitals, but hereafter we maintain this notation for simplicity.

When the triplet MOs are employed in the DDCI calculations, the resulting J values are largely underestimated with respect to the experimental ones, as shown in Table 2. This result is particularly surprising for $Cu_2(OH)_2$ because previous studies with the same methodology have provided good agreement with the experimental J value.[19,49,50] The only difference between these studies and this work is the Cu basis set. The incorporation of the f basis functions has been related to a slight underestimation of J on previous studies.[51] The marked effect found here will be discussed in a forthcoming paper, here we will focus on the impact of the nature of the MOs and of the size and composition of the active spaces on J.

Table 2 Magnetic coupling constants J (in cm^{-1}) at DDCI(2/2) level with different sets of MOs

	bisOH	$Cu_2(OH)_2$
Triplet MOs	−109	−350
Natural CAS + S MOs	−125	−394
Natural DDCI MOs	−150	−493
J_{exp}	−210	−509

Regarding the nature of the MOs, the question of whether the CASSCF MOs are well suited for variational or perturbation treatments of electron correlation in magnetic systems has been previously raised by different authors.[52–54] In perturbation treatments, the use of a minimal active space CASCI zeroth-order wave function with triplet (or singlet) orbitals usually gives underestimated values of J. A generally accepted strategy for obtaining better results is to extend the CAS with a set of virtual d-orbitals (introducing the radial correlation of the 3d electrons) and a few selected occupied ligand orbitals, which partially introduce at zeroth-order the effects brought about by Q9 LMCT.[16,55–57] Alternatively, it is possible to rely on the minimal active space if optimized (not in terms of the lowest energy) MOs are employed to build the reference wave functions, such as those resulting from the diagonalization of an average density matrix built from the two lowest CASSCF singlet states, mainly neutral and ionic in nature.[52] This procedure gives magnetic MOs which are more delocalized on the ligands, leading to a stabilization of the ionic forms, thus reducing U, and to an increase of the hopping integral between the magnetic orbitals. They resemble the natural DDCI orbitals and result in a significant improvement in the CASPT2 and NEVPT2 results.[52,58]

Among variational treatments, the DDCI J values have been traditionally considered highly independent of the MOs, with the exception of organic conjugated biradicals, where DDCI calculations on the basis of a minimal active space produce very poor results and an optimized set of MOs is required to obtain quantitative results.[52,53]

To this aim, two MO sets have been generated, the natural MOs obtained by the diagonalization of the average density matrix computed from the CAS(2,2) + S and from the DDCI wave functions. Table 2 reports the J values obtained with these two sets of MOs at the DDCI(2,2) level. The use of the natural DDCI MOs significantly improves the result for the bisOH system and gives a quantitatively correct estimate of J for the $Cu_2(OH)_2$ compound. The impact of the MO set is then noticeable and somewhat unusual for the DDCI approach, that is to say larger than what has been reported so far.

Fig. 3 and 4 show the magnetic orbitals of the natural DDCI MO set for the bisOH and $Cu_2(OH)_2$ molecules, respectively. One may qualitatively note that, compared to the corresponding triplet CASSCF MOs (Fig. 2), these orbitals are more delocalized on both the ethylendiamine ligand and on the bridging hydroxy group(s). Indeed, it is well known that natural orbitals partially describe the delocalization of the active electrons on the ligand orbitals.[20,59,60] Such a difference between the mean field singly occupied orbitals and the natural orbitals of a correlated wave function is also observed in complexes with only one metal center and in recent works,[61,62] it has been explained as a different composition of the wave function in OVB terms. In particular, the mean field approach (here CASSCF(2,2)) attributes an excessively large weight to the OVB structure with the unpaired electron on the metal center. Moreover, the importance of metal–ligand delocalization has also been invoked as a key ingredient in the non-orthogonal CI (NOCI) approach,[63–65] first applied to the prediction of magnetic couplings in La_2CuO_4 by Van Oosten *et al.*[66,67]

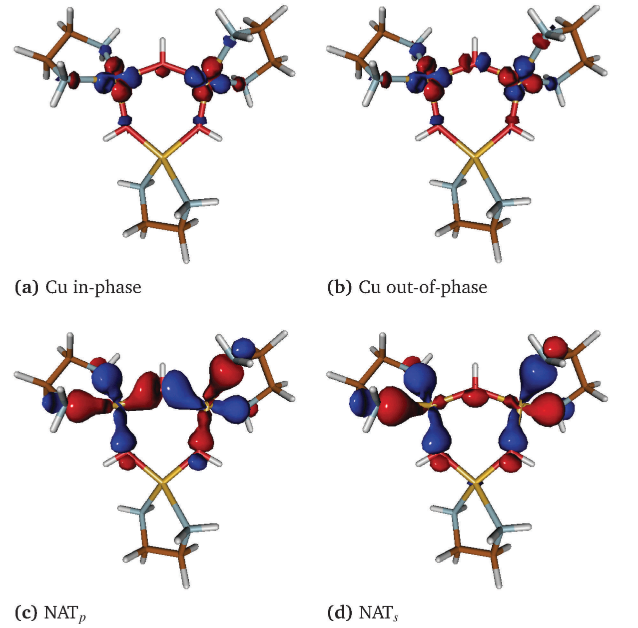

Fig. 3 Natural orbitals for bisOH from the average density matrices of the DDCI singlet and triplet wave functions: (a) and (b) magnetic orbitals, (c) and (d) ligand centered natural orbitals antisymmetric and symmetric with respect to the OH axis.

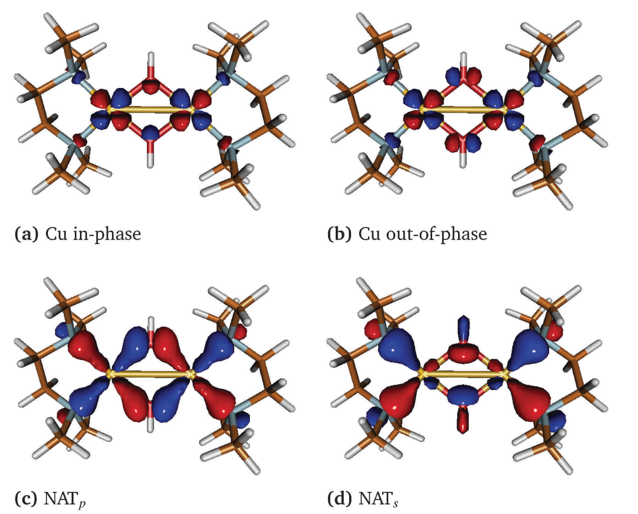

Fig. 4 Natural orbitals for $Cu_2(OH)_2$ from the average density matrices of the DDCI singlet and triplet wave functions: (a and b) magnetic orbitals, (c and d) ligand centered natural orbitals antisymmetric and symmetric with respect to the OH axis.

The results in Table 2 indicate that by using optimized MOs it is possible to obtain a good value of J for $Cu_2(OH)_2$, while for the bisOH system, at best only 70% of the experimental value is recovered. Actually, this is not an isolated case, similar behaviour can be found for other binuclear transition metal complexes.[16,52] Looking in detail at the characteristics of both systems, besides the number of bridges, the main differences come from: (i) the Cu–Cu bond distances (3.0 Å in $Cu_2(OH)_2$ and 3.69 Å in bisOH); (ii) the Cu–OH–Cu bond angle, 105° in $Cu_2(OH)_2$ and 140° in bisOH, and (iii) the coordination polyhedron of the Cu centers, square-planar for $Cu_2(OH)_2$ and slightly distorted square-planar in the bisOH molecule.

As a consequence of these structural differences, the OH group in bisOH acquires special relevance. To check whether the OH bridge is conveniently represented in the active space, we decided to extend the active space to two orbitals mainly located on the hydroxy group(s). Two different OH orbitals are relevant in this case, those able to overlap with the in-phase and out-of-phase combinations of the magnetic 3d orbitals, that is the sp hybrid orbital aligned with the O–H bond, and the O $2p_z$ orbital, aligned with the Cu–Cu axis.

Different approaches can be conceived to identify the MOs needed to extend the CAS. One possibility is to use the occupation numbers of the natural orbitals as a criterion to identify the extra orbitals. The two occupied orbitals with the largest deviation with respect to a double occupation (NAT_s and NAT_p) are presented in Fig. 3c and d for bisOH and Fig. 4c and d for $Cu_2(OH)_2$. NAT_s is symmetric with respect to the OH axis, while NAT_p is antisymmetric.

Two CI spaces have been explored, a CAS(6,4) + S space with all the 1h, 1p and 1h1p excitations with respect to the CAS(6,4), and the CAS(6,4) + DDC2 space, including also the double excitations involving two active orbitals (*i.e.* the 2h and 2p determinants). This strategy has been proposed in the past as an alternative to DDCI for systems where the DDCI space is too huge and the calculation becomes unfeasible.[50,60,68] When applied to our systems, this strategy has a different effect on the two systems considered (Table 3). In the case of $Cu_2(OH)_2$, the behavior is the same as that found in previous studies. The results obtained with the extended CAS are around the experimental value, representing 90% to 110% of the accepted value. In the case of bisOH, the situation is different. The extended CAS enhances the AF coupling and improves the agreement with the expected J value, but the agreement with the experimental value remains not fully satisfactory.

Instead of using the occupation number as a criterion, it is possible to localize a whole set of DDCI natural orbitals (with the Lewis procedure) and select those orbitals with a significant weight on the bridge(s). The resulting localized MOs are depicted in Fig. 5 and 6 for bisOH and $Cu_2(OH)_2$, respectively. The MOs labelled as L_s and L_p correspond to those with a large weight on the O sp hybrid and the O $2p_z$ orbitals, or in their out-of-phase combinations in the case of $Cu_2(OH)_2$. The L_s and L_p orbitals are symmetric and antisymmetric with respect to the O–H axis, respectively. The localization also facilitates the identification of the *core* and *virtual* orbitals that can be safely frozen and deleted, respectively, thus reducing the computational cost of these calculations.

The results obtained with this extended CAS, are almost stable for $Cu_2(OH)_2$ with respect to the DDCI(2,2), as shown in Table 3, while they are nicely improved for bisOH. In particular, at the CAS(6,4) + DDC2 level, the J values obtained with the

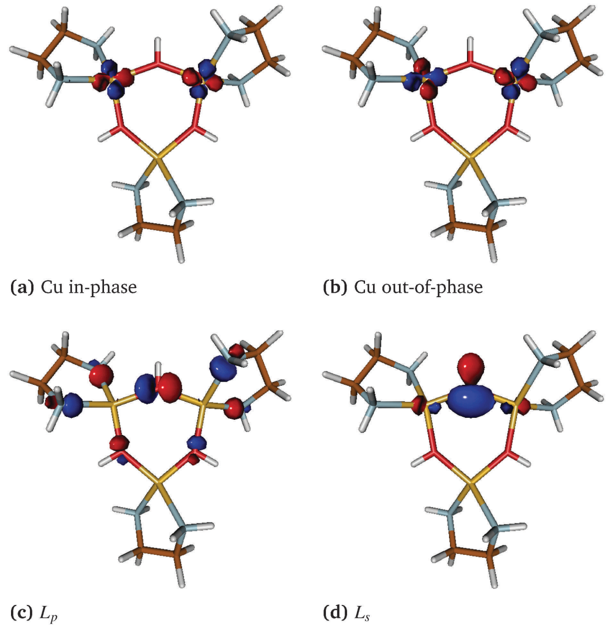

Fig. 5 Localized most relevant orbitals for bisOH (Lewis procedure on natural DDCI MOs set, see text).

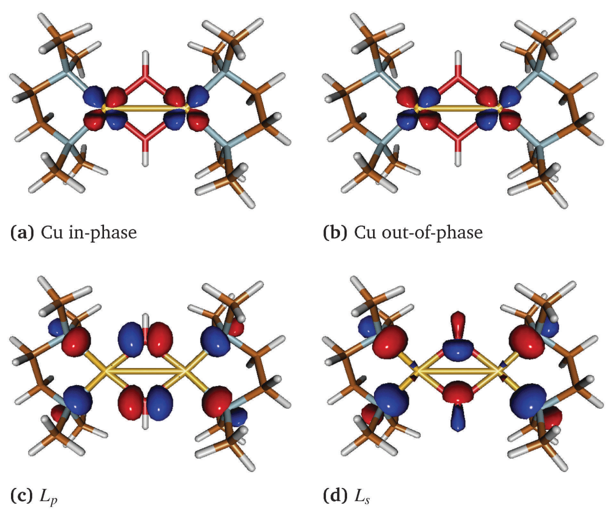

Fig. 6 Localized most relevant orbitals for $Cu_2(OH)_2$ (Lewis procedure on natural DDCI MOs set, see text).

Table 3 Magnetic coupling constants J (in cm^{-1}) using extended CAS and Lewis localized natural DDCI MOs

		bisOH	$Cu_2(OH)_2$
Delocalized MOs	CAS(6,4) + S	−205	−462
	CAS(6,4) + DDC2	−175	−568
Localized MOs	CAS(6,4) + S	−212	−447
	CAS(6,4) + DDC2	−232	−522
J_{exp}		−210	−509

localized DDCI natural MOs agree with the experimental values for both systems. The main difference with respect to the delocalized set comes from the bisOH system, where the use of localized bridging orbitals significantly improves the J estimates at both levels. This can be related to the localization procedure, which allows for larger control of the nature of the MOs included in the active space. In the case of $Cu_2(OH)_2$, after localization the two extra orbitals maintain essentially the same shapes as the delocalized ones, but the tails on Cu 3d orbitals have been eliminated and the weight on OH has slightly increased. In the case of bisOH, the delocalized ligand orbitals have a dominant weight on N, in particular for the NAT_s one (Fig. 3d), while the weight on OH is negligible. The origin of this difference can be found in the structural characteristics of bisOH, with the tetrahedral distortion of the Cu coordination sphere that places the N and OH ligands in different molecular planes, and the larger Cu–OH–Cu angle (140° *vs.* 105° in $Cu_2(OH)_2$) that reduces the overlap between the O sp hybrid and the Cu $3d_{x^2-y^2}$ orbitals. The localization allows us to select a well defined MO on the bridge, for both symmetries, but it is important to keep in mind the differences between the L_s orbitals of the two systems, which will have implications on the dominant magnetic pathways, as discussed in next section.

In summary, the use of an extended active space on the basis of the localized MOs seems to be a key ingredient for obtaining quantitative agreement with the experimental J value in the bisOH system. To explore the origin of this effect, an orthogonal valence-bond analysis of the CAS(6,4) + DDC2 wave functions was performed for both systems. It is worth noting that during the OVB analysis, for practical purposes, orthogonal atomic 3d orbitals were used, instead of the in-phase and out-of-phase combinations of them, as shown in the previous

Table 4 OVB structures and their energies. The energy of the neutral determinant is taken as the reference

Type	Structure	Determinant	Degeneracy	Energy (eV) bisOH	Energy (eV) $Cu_2(OH)_2$
Neutral	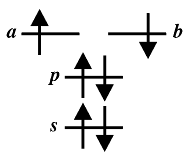	$\|s\bar{s}p\bar{p}a\bar{b}\|$	2	0.00	0.00
Ionic	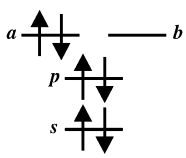	$\|s\bar{s}p\bar{p}a\bar{a}\|$	2	23.96	25.25
CT p	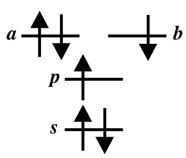	$\|s\bar{s}p\bar{a}a\bar{b}\|$	4	13.11	11.29
CT s	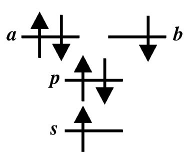	$\|s\bar{a}p\bar{p}a\bar{b}\|$	4	29.04	12.67
Double CT p	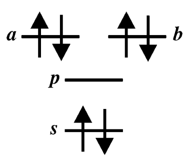	$\|s\bar{s}a\bar{a}b\bar{b}\|$	1	24.96	21.36
Double CT s	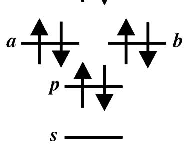	$\|p\bar{p}a\bar{a}b\bar{b}\|$	1	60.73	24.06
Mixed CT	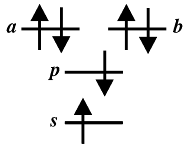	$\|s\bar{p}a\bar{a}b\bar{b}\|$	2	40.07	22.11

figures. This does not change in any way the results of the calculations.

4.2 Orthogonal valence-bond analysis

In the following, an orthogonal valence-bond analysis of the CAS(6,4) + DDC2 wave functions is performed for the bisOH and $Cu_2(OH)_2$ systems using the Lewis localized average natural orbitals.

The CAS(6,4) space consists of sixteen different OVB Slater determinants (indicated also with the term "structures" or "forms" in the following) of four different types: *neutral*, *ionic*, *charge transfer* and *double charge transfer*. Calling a and b the 3d active orbitals localized on the Cu atoms and s and p the L_s and L_p orbitals of the bridge (or their combinations in the case of $Cu_2(OH)_2$), the neutral determinants are $\|s\bar{s}p\bar{p}a\bar{b}\|$ and $\|s\bar{s}p\bar{p}b\bar{a}\|$. These two determinants are degenerate and their in-phase and out-of-phase combinations identify a singlet and a triplet state, respectively. The ionic determinants are $\|s\bar{s}p\bar{p}a\bar{a}\|$ and $\|s\bar{s}p\bar{p}b\bar{b}\|$ and they show a charge separation between the two magnetic centers. Together with the neutral structures, they form the one-band model CAS(2,2). The other determinants of the CAS space are charge transfer structures, specifically LMCT, with a transfer of electrons from the bridge ligands to the Cu atoms. A representative of a single CT is $\|s\bar{s}p\bar{a}a\bar{b}\|$ and it refers to the excitation of a spin down electron from the p bridge orbital to the a metallic center. There are eight different single LMCT forms, considering the spin and the involved metallic center. The last four determinants are double LMCT forms: $\|s\bar{s}a\bar{a}b\bar{b}\|$ for a double CT from the p orbital, $\|p\bar{p}a\bar{a}b\bar{b}\|$ from the s orbital and $\|s\bar{p}a\bar{a}bb\|$, a mixed double CT involving both the s and p orbitals.

A graphical representation of these structures is reported in Table 4, together with the corresponding Slater determinants and their energy with respect to the energy of the neutral determinant. The ionic determinants are very high in energy in both systems, U being ~24–25 eV. The charge transfer structures have different energies depending on the system. For $Cu_2(OH)_2$, the double charge transfer forms have an energy similar to that of the ionic ones, while the energy of the LMCT structures, ΔE_{CT}, is definitely lower. In bisOH, on the contrary, the excitations involving the s orbital (LMCT s in the following, CT s for short) is much higher in energy than those involving the p orbital (LMCT p, or CT p for short). Indeed, the LMCT p is 13 eV above the neutral determinant, while this gap increases to 29 eV (even larger than U) in the case of the LMCT s. The double charge transfer involving the L_s orbital (DCT s) is particularly destabilized, by more than 60 eV. In fact, for the bisOH system all excitations involving the s orbital are higher in energy than in $Cu_2(OH)_2$ (they are almost twice the energy). This suggests that the s orbital is much lower in energy (more stabilized) in bisOH and that it plays a different role in the mechanism of the magnetic coupling in these systems.

The most important interactions between the 16 OVB structures are shown in Table 5. The K_{ab} and t_{ab} parameters are the same of the one-band model while the others are characteristic of an extended two-band model. In more detail:

- K_{ab}: the direct exchange between the magnetic orbitals, which is the interaction between the two neutral structures.
- t_{ab}: the hopping integral, which is the interaction between ionic and neutral determinants.
- t_{CT}^{N}: the interaction between a neutral determinant and the LMCT. Two different terms can be distinguished depending on the type of ligand orbital (s or p) involved in the CT, labelled as CT s or CT p, respectively. The interaction is strong only when the unpaired electrons on the Cu atom and on the ligand have the same spin in the LMCT and in the neutral determinants, or in other words, when they are connected by a single-excitation.
- t_{CT}^{I}: the interaction between an ionic determinant and the LMCT. As in the previous case, there is a strong interaction only when they are connected by a single-excitation, that is, when the same Cu atomic orbital is doubly occupied in both determinants.
- t_{CT}^{DCT}: the interaction between the double charge transfer and LMCT forms. In this case, the value is the same for all LMCT forms.

From Table 5 one can note that K_{ab} and t_{ab} are relatively small compared to the other terms. Indeed, the LMCTs show a strong interaction with the ionic and neutral determinants, highlighting their fundamental role in the description of the physics of the system. In bisOH the interactions involving the

Table 5 Absolute values of the main interactions (in eV) in the CASCI(6,4) matrix on the basis of the OVB determinants

		Interaction (eV)	
Name	Matrix element	bisOH	$Cu_2(OH)_2$
K_{ab}	$\langle ssppab\|\hat{\mathscr{H}}\|ssppba\rangle$	0.02	1×10^{-3}
t_{ab}	$\langle ssppab\|\hat{\mathscr{H}}\|ssppaa\rangle$	0.72	0.03
$t_{CT\ p}^{N}$	$\langle ssppab\|\hat{\mathscr{H}}\|sspaab\rangle$	2.97	3.17
$t_{CT\ s}^{N}$	$\langle ssppab\|\hat{\mathscr{H}}\|sappab\rangle$	1.55	3.24
$t_{CT\ p}^{I}$	$\langle ssppaa\|\hat{\mathscr{H}}\|sspbaa\rangle$	1.36	2.03
$t_{CT\ s}^{I}$	$\langle ssppaa\|\hat{\mathscr{H}}\|sbppaa\rangle$	0.62	1.35
$t_{CT\ p}^{DCT\ p}$	$\langle sspbaa\|\hat{\mathscr{H}}\|ssaabb\rangle$	2.59	3.24
$t_{CT\ s}^{DCT\ s}$	$\langle sbppaa\|\hat{\mathscr{H}}\|ppaabb\rangle$	1.09	3.25

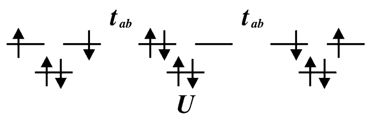

(a) Kinetic exchange

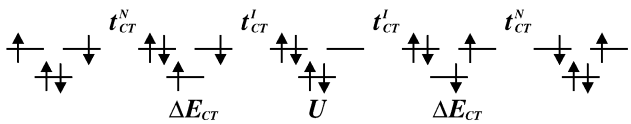

(b) Superexchange

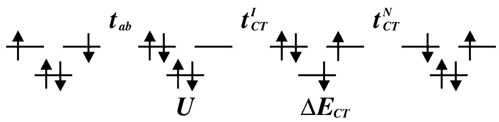

(c) Third-order through the ionic forms

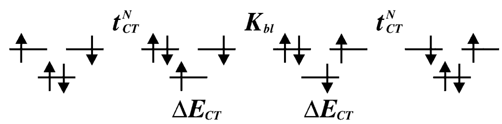

(d) Third-order through the exchange K_{bl} integral

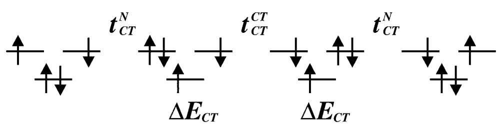

(e) Third-order through the hopping between the LMCT forms

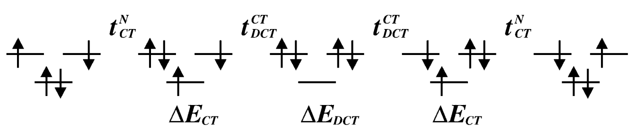

(f) The Goodenough mechanism, involving doubly charge transfer forms

Fig. 7 Main pathways governing the magnetic interaction.

ligand L_s orbital are smaller than the corresponding parameters concerning the L_p orbital. All interactions, with the exception of K_{ab} and t_{ab}, are larger in $Cu_2(OH)_2$ than in bisOH, in agreement with the relative values of their magnetic coupling constants.

The knowledge of these parameters allows the identification of the main pathways governing the magnetic interaction. In the one-band model, J can be calculated using the well-known equation

$$J = 2K_{ab} - \frac{4t_{ab}^2}{U} \quad (3)$$

where the first term is a ferromagnetic contribution that takes into account the direct exchange between the neutral forms (K_{ab} always being positive) and the second term is antiferromagnetic and considers the kinetic exchange through the ionic determinants, as shown in Fig. 7a.

It is well-known that this one-band model involving only the ionic and neutral determinants significantly underestimates the J value. The deviation is particularly severe in those systems where the active centers are far apart from each other, and both the kinetic and direct exchanges are negligible. The model then needs to explicitly introduce the ligand orbitals, leading to a two-band model. In this model, other interaction paths are conceivable and some of them are of key importance. For instance, the superexchange path that involves, besides the ionic structures, the LMCT forms (see Fig. 7b) plays a crucial role for a correct description of the energy splitting.

The contribution to the magnetic coupling is antiferromagnetic, and it depends on the hopping integrals, $t^{\mathrm{N}}_{\mathrm{CT}}$ and $t^{\mathrm{I}}_{\mathrm{CT}}$, following:

$$J \leftarrow -4\frac{\left(t^{\mathrm{N}}_{\mathrm{CT}}\right)^2 \cdot \left(t^{\mathrm{I}}_{\mathrm{CT}}\right)^2}{\Delta E^2_{\mathrm{CT}} \cdot U} \quad (4)$$

Depending on the nature of the ligand orbital, s or p, two different contributions can be distinguished, passing through the LMCT s or LMCT p forms. To return to the one-band model, these contributions can be included in an effective hopping integral, calculated as following:

$$t^{\mathrm{eff}}_{\mathrm{ab}} = t_{\mathrm{ab}} + \frac{4 \cdot t^{\mathrm{N}}_{\mathrm{CT}} \cdot t^{\mathrm{I}}_{\mathrm{CT}}}{\Delta E_{\mathrm{CT}}} \quad (5)$$

Since in bisOH t_{ab} does not have a negligible value, in this case it is possible to conceive also third-order pathways, as shown in Fig. 7c, which contributes to J as:

$$J \leftarrow 8\frac{t_{\mathrm{ab}} \cdot t^{\mathrm{I}}_{\mathrm{CT}} \cdot t^{\mathrm{N}}_{\mathrm{CT}}}{U \cdot \Delta E_{\mathrm{CT}}} \quad (6)$$

Two other third-order mechanisms are also possible, reported in Fig. 7d and e. Here, K_{bl} is the interaction between two LMCT structures only differing for the spins of the two unpaired electrons on the ligand l and metallic b orbitals. For l = p, the integral is $K_{\mathrm{bp}} = \langle \mathrm{sspaab}|\hat{\mathscr{H}}|\mathrm{ssbaap}\rangle$. $t^{\mathrm{CT}}_{\mathrm{CT}}$ is the interaction between two LMCT structures only differing on the doubly occupied Cu orbital, $t^{\mathrm{CT}}_{\mathrm{CT}} = \langle \mathrm{sspaab}|\hat{\mathscr{H}}|\mathrm{sspabb}\rangle$ contributing, respectively, by

$$J \leftarrow 4\frac{t^{\mathrm{N}}_{\mathrm{CT}} \cdot K_{\mathrm{bl}} \cdot t^{\mathrm{N}}_{\mathrm{CT}}}{\Delta E^2_{\mathrm{CT}}} \quad (7)$$

and by

$$J \leftarrow 4\frac{t^{\mathrm{N}}_{\mathrm{CT}} \cdot t^{\mathrm{CT}}_{\mathrm{CT}} \cdot t^{\mathrm{N}}_{\mathrm{CT}}}{\Delta E^2_{\mathrm{CT}}} \quad (8)$$

to the magnetic exchange. These contributions are proportional to the inverse of the energy of the charge transfer forms, therefore, for bisOH they are more important for the LMCT involving the p orbital than for those involving the s orbital.

Using energetic arguments, it is possible to also consider pathways involving the doubly ionic structures, or doubly charge transfer forms, known as the Goodenough mechanism in solid state physics,[69,70] as shown in Fig. 7f. Their contribution is:

$$J \leftarrow -8\frac{\left(t^{\mathrm{N}}_{\mathrm{CT}}\right)^2 \cdot \left(t^{\mathrm{CT}}_{\mathrm{DCT}}\right)^2}{\Delta E^2_{\mathrm{CT}} \cdot \Delta E_{\mathrm{DCT}}} \quad (9)$$

and similar expressions can be written for the pathways with mixed double charge transfer forms (MCT). The impact of each doubly ionic form on J will depend on their relative energies (Table 4). These energies are similar in the case of $Cu_2(OH)_2$, while only the DCT p structures are expected to play a significant role in the case of bisOH. It is worth noticing that most of these mechanisms involve the interaction between the LMCT and neutral forms, t_{CT}^{N}. If CASSCF triplet MOs are employed, this interaction t_{CT}^{N} in the CASCI matrix diminishes due to Brillouin's theorem,[18] since LMCTs are single excitations with respect to the neutral forms. However, when using natural MOs, these terms are far from negligible, as shown in Table 5. Hence, the Goodenough mechanism, usually considered as non-relevant due to the high energy of the doubly ionic form and the diminished interaction of the LMCT, is responsible for additional antiferromagnetic pathways when working with natural MOs. This role results in a non-negligible weight of the doubly ionic structures in the singlet wave function.

Other pathways are possible considering higher orders of perturbation. In an extended model such as the one considered here, one should evaluate hundreds of different paths. In the traditional DDCI procedure the diagonalization procedure takes into account all interactions at every possible order of perturbation. In this way one may obtain the correct J value but the physics of the system remains hidden. The use of the intermediate Hamiltonian theory allows one to overcome this problem.

For the systems studied in this work, the main model space (see Section 4.3) is clearly identified by the two degenerate neutral determinants. The identification of the intermediate model space is not straightforward. At a glance, the most natural choice is the rest of the CAS space: ionic, charge transfer and double charge transfer structures. Hence, the model space (main + intermediate) contains 16 determinants. Therefore, the outer space contains all other determinants of the CAS(6,4) + DDC2 space and using eqn (2) one may dress the 16 by 16 bare Hamiltonian matrix with the effect of the other determinants, which are 1 794 393 for bisOH and 792 324 for $Cu_2(OH)_2$.

The results obtained from the application of this procedure are shown in Table 6 (entries with $\tau = \infty$, *vide infra*). As one can see, the J value obtained from the diagonalization of the Hamiltonian in the full model space, J_{bare}, is not even qualitatively correct for bisOH, producing a ferromagnetic splitting. On the other hand, the diagonalization of the bare matrix dressed under the effect of the DDC2 space, provides correct magnetic behaviour (J_{Hint2} in Table 6) but the splitting is strongly overestimated for both systems.

In order to understand the reason why this procedure fails, one can look at the bare and dressed Hamiltonian matrix elements, reported in Table 7 ($B_{CAS(6,4)}$ and $D_{CAS(6,4)}$ columns, respectively). It is apparent that the ionic, CT and double CT structures withstand a very large stabilization by about 18, 12 and 16 eV, respectively. This large stabilization is the footprint of excitations contained in the outer space that strongly interact with the model space. In such a case, their effect cannot be treated through perturbation theory. To overcome this problem one has to include these excitations in the intermediate space, at the cost of losing the simplicity.

Table 6 Magnetic coupling constants (in cm^{-1}) obtained with different *brute-force* thresholds

System	τ	n. det	J_{bare}	J_{Hint2}
bisOH	∞	16	44.9	−1090.7
	0.010	208	29.43	−316.17
	0.009	220	11.00	−298.59
	0.008	232	11.00	−298.59
	0.007	250	−11.02	−255.50
	0.006	258	−11.18	−255.72
	0.005	274	−46.52	−217.41
	0.004	308	−46.99	−220.57
	0.003	438	−99.20	−168.73
	0.002	632	−99.48	−164.17
	0.001	1081	−108.98	−204.55
$Cu_2(OH)_2$	∞	16	−64.5	−1725.5
	0.020	128	−221.62	−357.20
	0.019	164	−39.04	−820.78
	0.018	176	−199.40	−516.74
	0.015	192	−204.02	−505.08
	0.009	212	−200.82	−494.16
	0.007	214	−227.81	−485.50
	0.005	222	−230.76	−484.53
	0.004	230	−233.53	−482.91
	0.003	374	−247.86	−481.17
	0.002	448	−255.73	−484.53
	0.001	883	−287.60	−520.41

Table 7 Bare (B) and dressed (D) Hamiltonian matrix elements (in eV) obtained using different model spaces: CAS(6,4) and the more extended CAS(6,4) + selected, where selected stands for d → d* + 1h N + 1h Cu 3d (see text)

System	Element	$B_{CAS(6,4)}$	$D_{CAS(6,4)}$	$D_{CAS(6,4)+selected}$
bisOH	E_0	0.0	0.0	0.0
	U	23.96	5.72	15.22
	$\Delta E_{CT\ p}$	13.11	2.12	7.71
	$\Delta E_{CT\ s}$	29.04	13.09	16.58
	$\Delta E_{DCT\ p}$	24.96	8.39	15.94
	$\Delta E_{DCT\ s}$	60.73	41.61	45.40
	ΔE_{MCT}	40.07	21.63	27.00
$Cu_2(OH)_2$	E_0	0.0	0.0	0.0
	U	25.19	7.78	18.10
	$\Delta E_{CT\ p}$	11.29	1.57	6.93
	$\Delta E_{CT\ s}$	12.67	2.84	8.09
	$\Delta E_{DCT\ p}$	21.36	4.94	13.49
	$\Delta E_{DCT\ s}$	24.06	8.26	16.41
	ΔE_{MCT}	22.11	6.03	14.54

Several ways to identify these determinants have been tested. A *brute-force* method consists of the definition of a threshold τ and in the inclusion in the model space of all the determinants of the outer space whose absolute perturbative contribution to a given matrix element of the model space is larger than τ, following the logic of the CIPSI algorithm.[71] Table 6 collects the results obtained with this method, ranked in order of decreasing τ. The first row with $\tau = \infty$ corresponds to a model space containing only the CAS(6,4) determinants. As the most important excitations are included in the model space, the large overestimation of J_{Hint2} is progressively corrected. The J_{bare} values gradually improve with the size of the space and they converge to the DDC2 values. However, the behaviour of J_{Hint2} is rather erratic, in particular for bisOH system. Different τ values are required to obtain a J_{Hint2} value of similar quality for both systems. The contributions are larger and concentrated in a smaller number of determinants in the case of $Cu_2(OH)_2$, while they are individually smaller and much more spread out in the case of bisOH.

Hence, the *brute-force* method solves the problem of over-stabilization of the structures in the model space but its dimension increases very fast and in an uncontrolled way, resulting in a difficult interpretation of the results. Actually, using a different selection procedure, it turns out that the number of determinants which have to be included in the model space is quite small and their nature well defined. One may describe these structures by both manually looking at the most important excitations in the *brute-force* method or using the orbital entanglement maps (*vide infra*), which allow one to identify the most important orbitals that are needed for the description of the system.

Entanglement, or mutual information, takes its roots in the field of quantum information theory and it has only recently been applied to quantum chemistry, especially in the framework of the Density Matrix Renormalization Group (DMRG), as a way to quantify orbital interactions.[72] In a given molecular system, one can define the entanglement between one orbital i and the other orbitals as the one-orbital von Neumann entropy:

$$s(1)_{\text{i}} = -\sum_{\alpha=1}^{4} \omega_{\alpha,\text{i}} \ln \omega_{\alpha,\text{i}} \tag{10}$$

where $\omega_{\alpha,\text{i}}$ are the eigenvalues of the one-orbital Reduced Density Matrix (RDM) corresponding to the 4 possible occupations of orbital i: 0, 1 (α or β spin) and 2 electrons. In the same way, one can define the two-orbital entropy from the eigenvalues ($\omega_{\alpha,\text{i,j}}$) of the two-orbital RDM:

$$s(2)_{\text{i,j}} = -\sum_{\alpha=1}^{16} \omega_{\alpha,\text{i,j}} \ln \omega_{\alpha,\text{i,j}} \tag{11}$$

This value quantifies the entanglement between the pair of orbitals i and j, and the other orbitals. If i and j are not entangled with each other, one has the equality $s(1)_{\text{i}} + s(1)_{\text{j}} = s(2)_{\text{i,j}}$. Therefore, the entanglement $I_{\text{i,j}}$ between the two orbitals can be defined as the deviation from this equality:

$$I_{\text{i,j}} = \frac{1}{2}\left[s(1)_{\text{i}} + s(1)_{\text{j}} - s(2)_{\text{i,j}}\right](1 - \delta_{\text{ij}}) \tag{12}$$

where the factor 1/2 prevents the double counting and δ assures that $I_{\text{i,i}} = 0$.

The quantity $I_{\text{i,j}}$ is often called ''mutual information'' because in some sense it represents how much the orbital i knows about orbital j. Starting from these values it is possible to obtain qualitative and quantitative information not only about the interaction between the orbitals and their roles in a given active space, but also about electron correlation effects and bond-formation processes.[73,74]

The entanglement maps of the triplet CAS(6,4) + DDC2 wavefunction for bisOH and $Cu_2(OH)_2$ are reported in Fig. 8 and 9, respectively. Similar maps are obtained for the singlet. The data have been obtained using a code recently developed by two of the authors of the present work (LT and CA). In the figures, each point corresponds to a localized orbital and the size of the red-dot is proportional to its one-orbital entropy. The color of the lines connecting two dots represents the magnitude of their entanglement: black if $I_{\text{i,j}} > 0.1$, green if $0.01 < I_{\text{i,j}} \leq 0.1$ and grey if $0.001 < I_{\text{i,j}} \leq 0.01$.

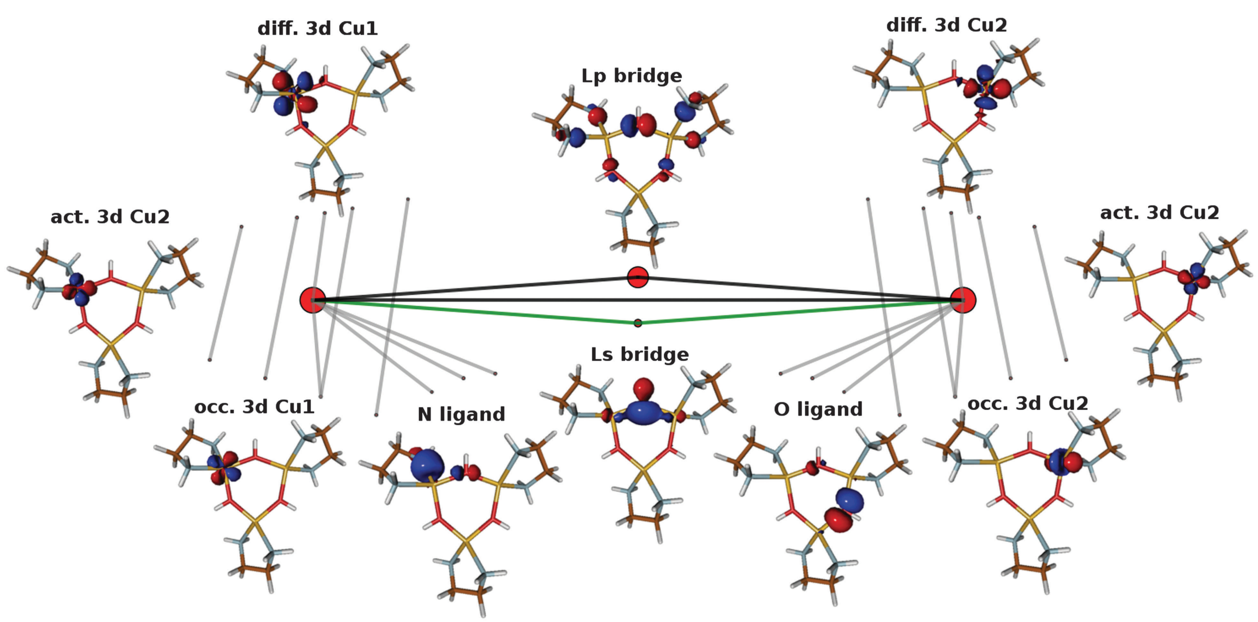

Fig. 8 Entanglement measures for bisOH. Triplet wavefunction, CAS(6,4) + DDC2.

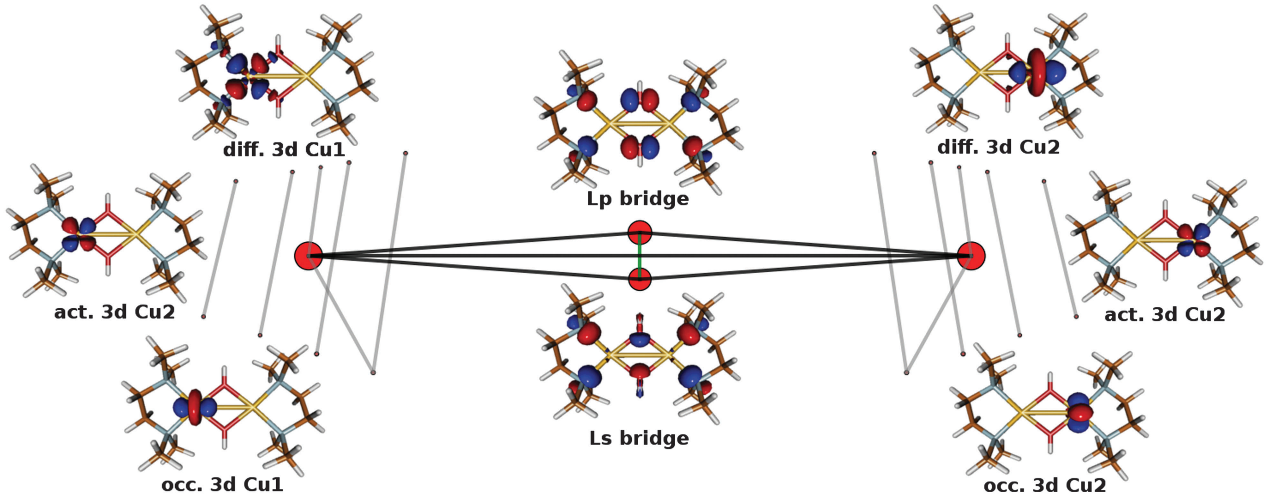

Fig. 9 Entanglement measures for $Cu_2(OH)_2$. Triplet wavefunction, CAS(6,4) + DDC2.

The orbitals reported are only those presenting a significant entanglement value. As one can see, besides the active orbitals, there are, for both bisOH and $Cu_2(OH)_2$, the non-active Cu 3d orbitals with their diffuse counterparts. Moreover, for bisOH, the occupied orbitals of both the nitrogen and the hydroxo ligands are also present. A strong entanglement between two orbitals means that they are involved in excitations that play a crucial role in the wave function. Thus, from the entanglement maps one can deduce a qualitative picture of the wave function. For instance, it is clear that for bisOH the L_p orbital plays a more important role than L_s, while for $Cu_2(OH)_2$ the two orbitals are almost equally important.

The entanglement maps help us identify (at least in the present case) a small but meaningful model space, showing the key role of a small number of 1h and 1h1p excitations in the description of the coupling:

(i) the single excitations from the non-active 3d Cu orbitals to their diffuse counterparts, in the following referred to as d → d* excitations. Each metallic center has four non-active 3d functions, resulting in eight different excitations per center.

(ii) the single excitations from the non-active Cu 3d orbitals to the active Cu 3d, referred to as 1h Cu 3d.

(iii) the single excitations from the lone pair N orbitals to the active Cu 3d orbitals. They correspond to ligand to metal charge transfer forms, labelled as 1h N, and seem to be important only for bisOH. It is worth noticing that these excitations introduce ligand-to-metal delocalization. In $Cu_2(OH)_2$ this delocalization is introduced *via* the L_s and L_p orbitals, both with a non-negligible weight on the lone pair N orbitals. In bisOH, however, only the L_p contains a certain weight on N. This can explain the different role of these excitations in both systems.

(iv) in minor extension, and only for bisOH, the single excitations from the neighbouring OH ligand orbitals to the active Cu 3d orbitals.

In principle, these excitations act on each determinant of the CAS(6,4) model space. However, after careful testing, the most important d → d* excitations are those acting on the CAS determinants with two electrons on the same magnetic Cu 3d orbital on which the excitation is applied. In other words, these structures correspond to local excitations on the ionic, LMCT and double charge transfer forms. With respect to the DDCI formalism on the basis of a minimal active space, these excitations belong to the 1h1p class when acting on the ionic forms, to the 2h1p set when acting on the CT forms, and to the 3h1p group if they act on the double charge transfer forms. They allow for orbital relaxation of the "overloaded" Cu center, promoting electrons from the occupied 3d shells to the diffuse ones, thus lowering the effective energy of the ionic and CT forms. This effect has been invoked in our previous analysis,[19] but here we provide numerical evidence of the impact of these excitations on magnetic coupling and evidence that these considerations are also corroborated by the entanglement measures. This selected set of d → d* excitations are the only ones considered for the enlargement of the model space. Different groups of these excitations have been added and the resulting model spaces are used in the intermediate Hamiltonian procedure. The so-obtained J values are shown in Table 8.

Table 8 Magnetic coupling constants (in cm^{-1}) obtained with the intermediate Hamiltonian theory using different model spaces

Model space	n. det	J_{bare}	J_{Hint2}
bisOH			
CAS(6,4)	16	44.9	−1090.7
CAS(6,4) + d → d*	176	8.39	−304.3
CAS(6,4) + d → d* + 1h Cu 3d	240	7.6	−311.9
CAS(6,4) + d → d* + 1h N	208	−11.6	−220.3
CAS(6,4) + d → d* + 1h N + 1h Cu 3d	272	−12.0	−229.1
CAS(6,4) + DDC2 (reference)	1 794 393	−231.6	—
$Cu_2(OH)_2$			
CAS(6,4)	16	−64.5	−1725.5
CAS(6,4) + d → d*	176	−199.4	−516.7
CAS(6,4) + d → d* + 1h Cu 3d	240	−199.4	−516.7
CAS(6,4) + d → d* + 1h N	208	−201.6	−515.9
CAS(6,4) + d → d* + 1h N + 1h Cu 3d	272	−201.6	−515.7
CAS(6,4) + DDC2 (reference)	792 324	−522.2	—

It is evident that the d → d* excitations have a key effect. When they are included in the model space, the diagonalization of the dressed Hamiltonian matrix produces quantitatively correct results, a coupling of $J = -516$ cm^{-1} for $Cu_2(OH)_2$, the expected value being -522 cm^{-1}, and $J = -304$ cm^{-1} for bisOH, still overestimated with respect to the CAS(6,4) + DDC2 value (-232 cm^{-1}). Looking at the Hamiltonian matrix elements within this space, it becomes obvious why these determinants must be included in the intermediate model space. Indeed, even if their energies are more than 50 eV higher than the neutral determinants, their interaction with the ionic and charge transfer structures is surprisingly large, being of the order of 5–6 eV. It is clear that it is not possible to treat an effect of this magnitude through a perturbation approach. The key role of these d → d* excitations can be related to the improvement usually observed in the CASPT2 evaluations of J when the minimal active space is extended with a set of formally virtual d-orbitals (referred as the 3d′ shell).[16,55–57] A similar effect of the d → d* excitations has also been recently observed in simple mononuclear Cu complexes, where the lowering of the LMCT energy and the corresponding increase in their coefficients in the wave functions has important consequences on their spin densities.[61,62] Actually, the key effect of d → d* excitations on magnetic coupling was originally predicted by the pioneering work of de Loth *et al.*,[6] but technical constraints at that time prevented a numerical evaluation through calculations using extended basis sets for Cu atoms.

The effect of the 1h Cu 3d is negligible for both systems, while the incorporation of the 1h N excitations has a marked effect for bisOH. Indeed, the J_{bare} value for bisOH becomes antiferromagnetic in nature, and the application of the intermediate Hamiltonian theory produces a quantitatively correct result for this system, $J = -220.3$ cm^{-1}. In the case of the $Cu_2(OH)_2$ system the impact of the 1h N excitations is negligible, in good agreement with the entanglement measurements. These excitations introduce ligand-to-metal delocalization, and the origin of their differential role on these systems can be found in the distinct weight of the N lone pairs on the L_s and L_p orbitals. In other words, these 1h N excitations correct the defective ligand-to-metal delocalization of the L_s orbital in bisOH. Notice that the quantitative evaluation of J in bisOH requires both an orbital with a large weight on the OH bridge and a correct description of the delocalization of the N lone pair orbitals. Finally, if both the 1h Cu 3d and 1h N are included in the model space, together with the d → d* excitations, the J values for both systems are close to the fully variational values.

Regarding the performance of the method, it is worth noting that a reduced number of determinants (272) provides estimates of the magnetic coupling that match the variational values obtained from a space containing 1–2 million determinants. This strategy, based on the perturbative dressing of a rationally selected model space and the subsequent diagonalization, can be envisaged as a promising approach for dealing with more complex systems, containing several magnetic centers with several active electrons, and as an alternative to pure variational approaches, which are usually too demanding for polynuclear compounds, and to DFT approaches showing the well-known dependence on the chosen functional.

A few (relevant) elements of the dressed matrices for this selected model space are shown in Table 7, more details can be found on the ESI† (Fig. S1 and S2). Comparing these values with those of the bare CAS(6,4), the largest changes occur on the relative energies of the neutral, ionic and CT forms, the modifications of the interaction parameters being less significant. There is a large stabilization of the ionic structures with respect to the neutral ones, resulting in a lowering of the U parameter. Also, the LMCT forms show a large lowering in the energy. In both cases, the magnitude of this effect is less extreme than that observed with the CAS(6,4) model space. The overall decrease of the energy of these structures clearly indicates their fundamental role in the description of the splitting. One may say that the effective work of the outer space is to stabilize these determinants in such a way that they can take on more importance in the wave function and correctly describe the physics of the system. The outer space consists essentially of single excitations that, when applied to the model space, can be seen as an orbital relaxation effect which lowers the energy of ionic structures. It should also be remarked that in the LMCT structures one of the metallic centers bears two electrons, resulting in an ''ionic'' nature.

In light of these results, it is possible to reconsider the different coupling pathways discussed above. Table 9 contains the individual contributions to the J_{Hint2} value of the mechanisms previously described in the frame of the two-band model. The evaluation of each contribution follows eqn (3)–(9), but using the interaction parameters of the dressed, ''rationally'' selected, model space. It is worth noting that this small number Q11

Table 9 Magnetic pathways and contributions to J_{Hint2} (in cm^{-1}) for the CAS(6,4) + selected model space

Pathway	Type	bisOH	$Cu_2(OH)_2$
$2K_{ab}$		82.3	−9.7
N–I–N		−884.4	0.006
N–CT–I–CT–N	p	−610.5	−1684.1
	s	−1.4	−569.2
	s–p	+58.1	+1958.1
N–CT–I–N	p	+1469.6	−6.2
	s	−69.9	+3.6
N–CT–CT–N *via* t_{ab}'	p	+1695.1	−330.9
	s	−52.0	+225.3
N–CT–CT–N *via* K_{bl}	p	+345.3	+249.2
	s	−13.0	+420.4
N–CT–DCT–CT–N	p	−2468.7	−7512.0
	s	−4.5	−4044.5
N–CT p–MCT–CT p–N	p	+130.5	+3194.8
N–CT s–MCT–CT s–N	s	+28.6	+2389.0
N–CT s–MCT–CT p–N	s–p	+122.2	+5525.3
Total		−172.7	−190.9

of contributions provides a significant fraction of the total J value, which means that a reduced number of pathways involving only the CAS(6,4) determinants condenses the main physics effects described by the CAS(6,4) + DDC2 calculation with almost 2 million determinants, and then, many more pathways of higher order. The results confirm the differential role of the LMCT s in these two systems: the pathways involving the LMCT s have a similar impact as those involving the LMCT p for $Cu_2(OH)_2$, while for bisOH the LMCT s are significantly less important for the coupling than the LMCT p. The large interaction between the ionic and neutral forms in bisOH is also crucial, enhancing all pathways involving this interaction. Such a term is almost negligible for $Cu_2(OH)_2$. Third-order pathways show different signs for L_p and L_s: they almost compensate for each other in $Cu_2(OH)_2$, while they introduce an important ferromagnetic contribution in the case of bisOH. Indeed, neglecting all pathways involving the LMCT s gives a J value of $-240\ cm^{-1}$ for bisOH. Finally, as mentioned above, the double ionic forms play a significant role in these two systems, an effect which could be partially ascribed to the use of natural MOs.

5 Conclusions

In this work, we have applied a combined *perturbative + variational* strategy to the evaluation of the magnetic coupling constants in two antiferromagnetic systems. The method makes use of an OVB reading of the wave functions and the intermediate Hamiltonian theory to select the set of key excitations which need to be treated variationally together with the determinants of an extended active space. These key excitations represent just a very small fraction (less than 0.05%) of the whole CI space, but, once dressed, provide J values that quantitatively reproduce the experimental ones.

The importance of this strategy is then twofold: (i) it is possible to quantitatively estimate the coupling constants at very low-cost, essentially the cost of the diagonalization of a matrix with a few hundred determinants, and (ii) it is possible to isolate and characterize the main excitations contributing to the coupling. Concerning this point, entanglement maps have proven to be a useful tool to identify the orbitals, and hence the excitations, which play a crucial role in the coupling.

The interaction between the LMCT, 1h1p and 2h1p excitations have been implicated in our previous studies as responsible for the performance of the DDCI approach when dealing with antiferromagnetic systems.[17–20] Here, we have demonstrated that among all 1h1p and 2h1p excitations contained in the rather large DDCI space, those with a key role are the local $d \rightarrow d^*$ excitations, which introduce the relaxation of a 3d shell completely filled in the ionic and charge transfer forms. This result agrees with recent studies by Giner and Angeli[61,62] on the impact of these excitations on the correct description of the spin density.

The procedure requires the use of optimized molecular orbitals, which are localized prior to the OVB reading of the wave functions. Besides the satisfactory evaluation of J, the method also provides values for the interaction parameters among the determinants of the model space, which allow for the identification of the main pathways controlling the coupling.

Regarding the two molecular systems considered here, this study goes some way to explaining the difficulties encountered by Vancoillie *et al.*[29] in their previous estimation of the coupling in the parent trisOH compound. First, the use of an extended active space, including the bridging OH orbitals is compulsory, the OMs need to be optimized to correctly introduce metal–ligand delocalization and finally, the Cu basis functions display a non-negligible and surprisingly high effect.

In summary, the work reported here can be considered as a first step towards a general tool to deal with polynuclear systems containing localized spin moments and systems where calculations based on a minimal active space fail to quantitatively reproduce the magnetic coupling constant, as for many ferromagnetic systems.[75] Further work is needed to optimize the molecular orbital sets in a simple and low-cost way. In this regard, the recent proposal by Giner and Angeli[62] for orbital optimization in open-shell systems seems to be a promising route. Once this issue has been addressed, the *perturbative + variational* strategy proposed here could pave the way for a general and powerful approach for studying complex systems and close the gap between the systems proposed by experimentalists and those that can be successfully described by affordable state-of-the-art quantum chemistry methods.

Acknowledgements

C. J. C. is thankful for the support of the Universidad de Sevilla, Spain, and the technical support of the Supercomputing Team of the Centro Informático Científico de Andalucía (CICA). C. A. and L. T. acknowledge the support of the University of Ferrara which has sponsored their research stay at the U. Sevilla within the projects MolMagRes (C. A.) and ''Bando Giovani Ricercatori 2015'' (L. T.), funded by 5 per mille dell'IRPEF a sostegno della Ricerca dell'Università di Ferrara. D. M. thanks the Laboratoire de Chimie et Physique Quantique (U. Toulouse/CNRS) for supporting his research stay at the U. Sevilla.

References

1 P. W. Anderson, *Phys. Rev.*, 1950, **79**, 350.
2 O. Kahn and B. Briat, *J. Chem. Soc., Faraday Trans. 2*, 1976, **72**, 268.
3 P. J. Hay, J. C. Thibeault and R. J. Hoffmann, *J. Am. Chem. Soc.*, 1975, **97**, 4884.
4 P. de Loth, P. Cassoux, J.-P. Daudey and J.-P. Malrieu, *J. Am. Chem. Soc.*, 1981, **103**, 4007.
5 M. Charlot, M. Verdaguer, Y. Journaux, P. de Loth and J. Daudey, *Inorg. Chem.*, 1984, **23**, 3802.
6 P. de Loth, J. Daudey, H. Astheimer, L. Walz and W. Haase, *J. Chem. Phys.*, 1985, **82**, 5048.

7 P. de Loth, P. Karafiloglou, J. Daudey and O. Kahn, *J. Am. Chem. Soc.*, 1988, **110**, 5676.
8 C. J. Calzado, J. M. Clemente-Juan, E. Coronado, A. Gaita-Ariño and N. Suaud, *Inorg. Chem.*, 2008, **47**, 5889.
9 C. de Graaf and F. Illas, *Phys. Rev. B: Condens. Matter Mater. Phys.*, 2001, **63**, 014404.
10 C. de Graaf, I. de, P. R. Moreira, F. Illas, O. Iglesias and A. Labarta, *Phys. Rev. B: Condens. Matter Mater. Phys.*, 2002, **66**, 014448.
11 F. Nepveu, W. Haase and H. Astheimer, *J. Chem. Soc., Faraday Trans. 2*, 1986, **82**, 551.
12 H. Astheimer and W. Haase, *J. Chem. Phys.*, 1986, **85**, 1424.
13 J. Miralles, J.-P. Daudey and R. Caballol, *Chem. Phys. Lett.*, 1992, **198**, 555.
14 J. Miralles, O. Castell, R. Caballol and J.-P. Malrieu, *Chem. Phys.*, 1993, **172**, 33.
15 R. Broer and W. J. A. Maaskant, *Chem. Phys.*, 1986, **102**, 103.
16 J. Malrieu, R. Caballol, C. J. Calzado, F. de Graaf and N. Guihery, *Chem. Rev.*, 2014, **114**, 429–492.
17 C. J. Calzado, J. Cabrero, J.-P. Malrieu and R. Caballol, *J. Chem. Phys.*, 2002, **116**, 2728.
18 C. J. Calzado, J. Cabrero, J.-P. Malrieu and R. Caballol, *J. Chem. Phys.*, 2002, **116**, 3985.
19 C. J. Calzado, C. Angeli, D. Taratiel, R. Caballol and J.-P. Malrieu, *J. Chem. Phys.*, 2009, **131**, 044327.
20 J. Cabrero, C. J. Calzado, D. Maynau, R. Caballol and J.-P. Malrieu, *J. Phys. Chem. A*, 2002, **106**, 8146.
21 T. Mitchell, W. Bernard and J. Wasson, *Acta Crystallogr., Sect. B: Struct. Crystallogr. Cryst. Chem.*, 1970, **26**, 2096.
22 L. M. Mirica and D. P. Stack, *Inorg. Chem.*, 2005, **44**, 2132–2133.
23 J. Yoon, L. M. Mirica, D. P. Stack and E. I. Solomon, *J. Am. Chem. Soc.*, 2004, **126**, 12586–12595.
24 J. Yoon and E. I. Solomon, *Inorg. Chem.*, 2005, **44**, 8076–8086.
25 J. Yoon, L. M. Mirica, T. D. P. Stack and E. I. Solomon, *J. Am. Chem. Soc.*, 2005, **127**, 13680–13693.
26 P. A. M. Dirac, *Proc. R. Soc. London, Ser. A*, 1926, **112**, 661.
27 W. Heisenberg, *Z. Phys.*, 1928, **49**, 619.
28 J. H. van Vleck, *Electric and Magnetic Susceptibilities*, Clarendon Press, Oxford, 1932.
29 S. Vancoillie, J. Chalupský, U. Ryde, E. I. Solomon, K. Pierloot, F. Neese and L. Rulšek, *J. Phys. Chem. B*, 2010, **114**, 7692–7702.
30 F. Aquilante, L. De Vico, N. Ferré, G. Ghigo, P.-Å. Malmqvist, P. Neogrady, T. B. Pedersen, M. Pitoňák, M. Reiher, B. O. Roos, L. Serrano-Andrés, M. Urban, V. Veryazov and R. Lindh, *J. Comput. Chem.*, 2010, **31**, 224.
31 OVB-Ferrara package developed at the Department of Chemical and Pharmaceutical Sciences, University of Ferrara, Italy.
32 C. Angeli, R. Cimiraglia and J.-P. Malrieu, *J. Chem. Educ.*, 2008, **85**, 150–158.
33 C. Angeli, R. Cimiraglia and J.-P. Malrieu, *Mol. Phys.*, 2013, **111**, 1069–1077.
34 CASDI package developed at the Laboratoire de Physique Quantique, Université Paul Sabatier, Toulouse, France.
35 N. Ben Amor and D. Maynau, *Chem. Phys. Lett.*, 1998, **286**, 211.
36 W. Wu, P. Su, S. Shaik and P. C. Hiberty, *Chem. Rev.*, 2011, **111**, 7557–7593.
37 S. Shaik and P. C. Hiberty, *A Chemist's Guide to Valence Bond Theory*, John Wiley & Sons, Inc., Hoboken, New Jersey, 2007.
38 J.-P. Malrieu, N. Guihéry, C. J. Calzado and C. Angeli, *J. Comput. Chem.*, 2007, **28**, 35–50.
39 C. Angeli, *J. Comput. Chem.*, 2009, **30**, 1319–1333.
40 C. Angeli, *Int. J. Quantum Chem.*, 2010, **110**, 2436–2447.
41 C. Angeli, C. J. Calzado, C. de Graaf and R. Caballol, *Phys. Chem. Chem. Phys.*, 2011, **13**, 14617.
42 J. M. Foster and S. F. Boys, *Rev. Mod. Phys.*, 1960, **32**, 303–304.
43 C. Edmiston and K. Ruedenberg, *Rev. Mod. Phys.*, 1963, **35**, 457–464.
44 J. Pipek and P. G. Mezey, *J. Chem. Phys.*, 1989, **90**, 4916–4926.
45 C. Angeli, S. Evangelisti, R. Cimiraglia and D. Maynau, *J. Chem. Phys.*, 2002, **117**, 10525–10533.
46 C. Bloch, *Nucl. Phys.*, 1958, **6**, 329–347.
47 J.-P. Malrieu, D. Maynau and J.-P. Daudey, *Phys. Rev. B: Condens. Matter Mater. Phys.*, 1984, **30**, 1817–1832.
48 J.-P. Malrieu, P. Durand and J.-P. Daudey, *J. Phys. A: Math. Gen.*, 1985, **18**, 809.
49 C. J. Calzado, S. Evangelisti and D. Maynau, *J. Phys. Chem. A*, 2003, **107**, 7581.
50 C. J. Calzado, C. Angeli, R. Caballol and J.-P. Malrieu, *Theor. Chem. Acc.*, 2010, **126**, 185.
51 D. Muñoz, C. de Graaf and F. Illas, *J. Comput. Chem.*, 2004, **25**, 1234–1241.
52 C. Angeli and C. J. Calzado, *J. Chem. Phys.*, 2012, **137**, 034104.
53 N. Suaud, R. Ruamps, N. Guihéry and J.-P. Malrieu, *J. Chem. Theory Comput.*, 2012, **8**, 4127–4137.
54 W. T. Borden, E. R. Davidson and D. Feller, *Tetrahedron*, 1982, **38**, 737.
55 B. H. Botch, T. H. Dunning Jr. and J. F. Harrison, *J. Chem. Phys.*, 1981, **75**, 3466.
56 K. Pierloot, *Int. J. Quantum Chem.*, 2011, **111**, 3291.
57 K. Andersson, P.-Å. Malmqvist and B. O. Roos, *J. Chem. Phys.*, 1992, **96**, 1218.
58 M. Spivak, C. Angeli, C. Calzado and C. de Graaf, *J. Comput. Chem.*, 2014, **35**, 1665–1671.
59 C. J. Calzado and J.-P. Malrieu, *Phys. Rev. B: Condens. Matter Mater. Phys.*, 2001, **63**, 214520.
60 A. Gellé, M. Munzarová, M. B. Lepetit and F. Illas, *Phys. Rev. B: Condens. Matter Mater. Phys.*, 2003, **68**, 125103.
61 E. Giner and C. Angeli, *J. Chem. Phys.*, 2015, **143**, 124305.
62 E. Giner and C. Angeli, *J. Chem. Phys.*, 2016, **144**, 104104.
63 R. Broer and W. C. Nieuwpoort, *Theor. Chim. Acta*, 1988, **73**, 405.
64 R. Broer, A. Van Oosten and W. C. Nieuwpoort, *Rev. Solid State Sci.*, 1991, **5**, 79.

65 R. Broer, L. Hozoi and W. C. Nieuwpoort, *Mol. Phys.*, 2003, **101**, 233.
66 A. B. van Oosten, R. Broer and W. C. Nieuwpoort, *Int. J. Quantum Chem., Symp.*, 1995, **29**, 241.
67 A. B. van Oosten, R. Broer and W. C. Nieuwpoort, *Chem. Phys. Lett.*, 1996, **257**, 207.
68 E. Bordas, R. Caballol, C. de Graaf and J.-P. Malrieu, *Chem. Phys.*, 2005, **309**, 259.
69 W. Geertsma, *Physica B*, 1990, **241**, 164.
70 H. Eskers and H. Jefferson, *Phys. Rev. B: Condens. Matter Mater. Phys.*, 1993, **9788**, 48.
71 B. Huron, J. P. Malrieu and P. Rancurel, *J. Chem. Phys.*, 1973, **58**, 5745–5759.
72 J. Rissler, R. M. Noack and S. R. White, *Chem. Phys.*, 2006, **323**, 519–531.
73 K. Boguslawski, P. Tecmer, O. Legeza and M. Reiher, *J. Phys. Chem. Lett.*, 2012, **3**, 3129–3135.
74 K. Boguslawski, P. Tecmer, G. Barcza, O. Legeza and M. Reiher, *J. Chem. Theory Comput.*, 2013, **9**, 2959–2973.
75 A. Ozarowski, C. J. Calzado, R. P. Sharma, S. Kumar, J. Jezierska, C. Angeli, F. Spizzo and V. Ferretti, *Inorg. Chem.*, 2015, **54**, 11916–11934.